MATEC Web of Conferences **14**, 15003 (2014)
DOI: 10.1051/matecconf/20141415003

Multi-scale modelling of Suzuki segregation in γ' precipitates in Ni and Co-base superalloys

P. Srimannarayana, K.V. Vamsi, and S. Karthikeyan[a]

Department of Materials Engineering, Indian Institute of Science, Bangalore 560012, India

Abstract. The high temperature strength of alloys with $(\gamma + \gamma')$ microstructure is primarily due to the resistance of the ordered precipitate to cutting by matrix dislocations. Such shearing requires higher stresses since it involves the creation of a planar fault. Planar fault energy is known to be dependent on composition. This implies that the composition on the fault may be different from that in the bulk for energetic reasons. Such segregation (or desegregation) of specific alloying elements to the fault may result in Suzuki strengthening which has not been explored extensively in these systems. In this work, segregation (or desegregation) of alloying elements to planar faults was studied computationally in Ni_3(Al,Ti) and Co_3(W,Al) type γ' precipitates. The composition dependence of APB energy and heat of mixing were evaluated from first principle electronic structure calculations. A phase field model incorporating the first principles results, was used to simulate the motion of an extended superdislocation under stress concurrently with composition evolution. Results reveal that in both systems, significant (de)segregation occurs on equilibration. On application of stress, solutes were dragged along with the APB in some cases. Additionally, it was also noted the velocity of the superdislocation under an applied stress is strongly dependent on atomic mobility (i.e. diffusivity).

1. Introduction

Ni-base superalloys are extensively used in high temperature applications for their superior mechanical properties and oxidation resistance compared to other materials [1]. These alloys typically have a microstructure of coherent γ' ordered precipitates with $L1_2$ structure embedded in a FCC γ matrix. Recently, similar $(\gamma + \gamma')$ microstructures have also been reported in Co-base superalloys based on the Co-Al-W system [2]. The composition of γ' is typically Ni_3(Al,Ti,Ta) and Co_3(Al,W) in Ni-base and Co-base superalloys.

In both these superalloys, the primary glide dislocation in γ matrix has a Burgers vector of $\frac{1}{2} <101>$ on $\{111\}$ [1]. Since the $\frac{1}{2} <101>$ vector is not a lattice translation in γ', if a dislocation with this Burgers vector cuts through the precipitate, an Anti-Phase Boundary (APB) is created. APBs and other planar faults play an important role as their energy affects phenomena such as cross-slip and yield anomaly [1,3], recovery and strain hardening [3], creep [4], twinning [5] and strength of γ' precipitates [6].

Several studies [7–14] have shown that APB energy is strongly dependent on composition. Fault energy is the excess energy due to difference in the coordination environment experienced by an atom on the fault in comparison to an atom in the bulk. In a companion paper in this conference, Vamsi et al., have rationalized the variation of fault energy with composition in $Ni_3Al_{(1-x)}X_x$, (X=Ta, Ti) in terms of change in the number and type of nearest neighbor violations. The fault energy values can vary significantly in magnitude over the composition range and the functional form of variation is also dependent upon the alloying element.

Such a dependence of fault energy on composition is expected to significantly affect the aforementioned properties. Additionally, this dependence of interface energy on composition, suggests that the fault is likely to have a different composition than the bulk. From Gibb's adsorption isotherm [15], if addition of a solute reduces the interface energy (in a binary alloy), then there is a tendency for segregation of the solute to the interface, whereas, if the solute increases the interface energy, there is a tendency for desegregation. The phenomenon of segregation (or desegregation) of alloying elements to (or away from) planar fault is called Suzuki segregation [16]. For instance, in the case where a [011] super dislocation in γ' splits into two $\frac{1}{2}$ [011] partial dislocations separated by an APB, the equilibrium composition on the fault can be different from the overall γ' composition. While the dependence of APB energy on composition is well acknowledged, the possibility of Suzuki strengthening has not been addressed adequately in Ni- and Co-base super alloys.

Suzuki segregation can result in phenomena similar to those resulting from the presence of solute atmospheres near dislocations. At high temperatures, segregation (or desegregation) by diffusion is possible, resulting in the composition of the stacking fault achieving the equilibrium value dictated by Gibb's adsorption isotherm. The motion of the dislocation in this case will thus involve drag

[a] Corresponding author: karthik@materials.iisc.ernet.in

of solute atoms along with the stacking fault resulting in strengthening [17]. This effect is similar to drag of solute atmospheres by dislocations. In contrast, at low temperatures (i.e., low diffusivity), high stresses are required to break extended dislocations free of solute traps.

A variety of interesting phenomena can emerge when dislocation velocity and diffusion rates are comparable. For instance, when an external stress is applied to an extended dislocation, the leading and trailing partials experience different driving forces for motion, even if they have the same Burgers vector [16]. This could result in the trailing partial being pinned, while the leading partial moves leaving an extended stacking fault behind. The difference in the driving force depends on the relative mobility of the dislocation with respect to diffusion. While the extreme cases of diffusion rates $\gg$ dislocation velocity and diffusion rates $\ll$ dislocation velocities can be modeled analytically [16], more realistic scenarios involving competition between diffusion and dislocation motion are difficult to address. It is, in this context that we aim to probe these phenomena using phase field models.

While there is a large body of literature available on use of phase-field models to study dislocation motion [18–21], there is limited work on the study of solute atmospheres in the vicinity of dislocations [22–24]. While Suzuki segregation to infinitely-wide planar faults has been studied via phase field models in a Co-base alloy [25], to the best of the authors' knowledge, there is no literature on phase-field modeling of Suzuki segregation to planar faults that are limited by partial dislocations. Additionally, there is no existent literature on the effect of stress on movement of such extended dislocations. In this paper, we first outline the formulation of a 2D phase-field model for simulating Suzuki segregation and strengthening. This is followed by results from simulations on two pseudo-ternary γ' systems, viz. Ni_3(Al,Ti) and Co_3(Al,W).

2. Computational approach

In this paper, we present only the most relevant equations. A more detailed mathematical treatment will be presented elsewhere [26]. General details of phase-field based approach are available in several excellent reviews [27]. Phase field models are typically applied to problems dealing with diffuse interfaces, where a parameter (λ) which characterizes the phase varies continuously from one phase to another phase separated by an interface. The parameter is defined as a function of spatial coordinates and captures a specific feature of the microstructure. The parameter can be composition, grain orientation, magnetic spin, etc. [27].

The key equation in phase field modelling is obtained by expressing the free energy of heterogeneous system (i.e., spatially varying λ) as a Taylor series expansion about free energy of homogeneous system [28]. Using symmetry arguments and neglecting higher order terms except the first non-zero gradient term, the energy of the system can be written as:

$$E_{heterogeneous} = E_{homogeneous} + E_{gradient} \tag{1a}$$

$$E|_{\lambda} = E_o|_{\lambda} + \kappa_{\lambda} (\nabla\lambda)^2 . \tag{1b}$$

The evolution equation, i.e., how λ evolves with time, is obtained by using energy minimization arguments [29,30]. If λ is a non-conserved entity (such as grain orientation), then its evolution is given by the Allen-Cahn equation [30]:

$$\frac{\partial\lambda}{\partial t} = -M_{\lambda}\left(\frac{\partial E_o}{\partial\lambda} - 2\kappa_{\lambda}\nabla^2\lambda\right). \tag{2}$$

If λ is a conserved entity such as composition, evolution must account for flux of the parameter via a continuity equation. The resulting evolution equation is called Cahn-Hilliard Equation [29]

$$\frac{\partial\lambda}{\partial t} = -M_{\lambda}\nabla\cdot\left[-\nabla\left(\frac{\partial E_o}{\partial\lambda} - 2\kappa_{\lambda}\nabla^2\lambda\right)\right]. \tag{3}$$

For the problem at hand, the dislocation was modeled as an interface between the slipped and unslipped region. The phase field parameter is related to the relative displacement between upper half and lower half of the crystal. In the slipped region, the relative displacement is an integral multiple of Burgers vector (b) and in the unslipped region, the relative displacement is zero. We introduce a normalized slip parameter (η) as a phase field parameter for dislocation. "η" is defined as the ratio of the magnitude of relative displacement to that of magnitude of Burgers vector. Core of the dislocation is defined as the location where spatial derivative of relative displacement is highest. The parameter η is a non-conserved entity since during dislocation motion, slipped region increases and unslipped region decreases. In addition to η, which informs whether a region is slipped or unslipped, space is also characterized by a second phase field variable, i.e., composition (c) which is a conserved entity. In a pseudo-binary system such as Ni_3(Al,Ta), "c" corresponds to the composition of Ta in the Al sub-lattice.

In order to implement this model, the energy of the homogeneous system (E_o) needs to be described as function of the phase field parameters. Consider a system whose energy depends only on η, but not on c. One can write for a $1/2$ [110] single perfect dislocation:

$$E_o|_{\eta} = E_{\eta}|_{\max}\sin^2(\pi\eta) - \tau_{applied} b\eta. \tag{4}$$

The first term is related to the dislocation self-energy, ($E_{\eta}|_{max}$ is a constant that depends on line energy i.e., $\alpha\mu b^2$) while the second term is related to the work done by the external stress, $\tau_{applied}$. Here, μ is shear modulus, b is magnitude of Burgers vector, α accounts for the orientation of the dislocation. For a single $1/2$ [110] dislocation, $\eta = 0$ is the unslipped region and $\eta = 1$ is the slipped region.

Now for a pair of parallel straight $1/2$ [110] dislocations separated by an APB:

$$E_o|_{\eta} = E_{\eta}|_{\max}\sin^2(\pi\eta) - \tau_{applied} b\eta + E_{interaction}(\eta) + E_{APB}(\eta). \tag{5}$$

While the first two terms once again describe the dislocation line energy and the work done by applied

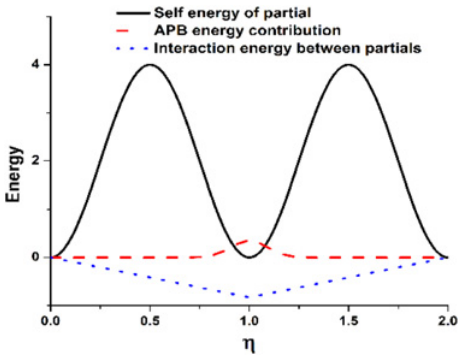

Figure 1. Variation of the various components of E_o with η for a pair of straight dislocations.

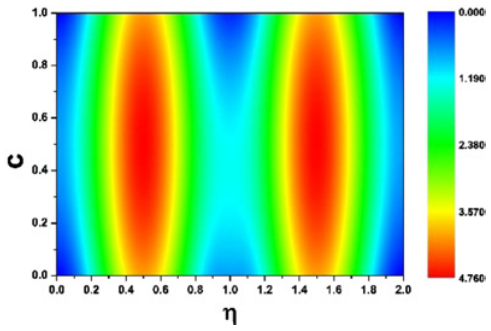

Figure 2. Variation of E_o as a function of c and η in a model system. Note that energy values here have been exaggerated for elucidation.

stress, one needs to account for two additional terms: $E_{interaction}$ which arises from the repulsive interaction between the super partial dislocations, and E_{APB} to account for the energy penalty due to the APB. The individual contributions to homogeneous energy for this system containing an extended superdislocation is shown in Fig. 1. In this case, $\eta = 0$ in the unslipped region, $\eta = 1$ corresponds to the APB and $\eta = 2$ corresponds to the region swept by both superpartial dislocations. Note that the maximum values of $E_{interaction}$ and E_{APB} as seen in Fig. 1 are:

$$E_{interaction}|_{\max} = \frac{\alpha \mu b^2}{2\pi d} \tag{6}$$

$$E_{APB}|_{\max} = \gamma|_{APB}. \tag{7}$$

Here, d is the separation between superpartial dislocations, which is monitored during the simulation and used to update the interaction energy at each time-step.

However, since we are interested in studying compositional variations, we need to write the energy of the homogeneous system as function of both c and η:

$$E_o|_\eta = E_\eta|_{\max} \sin^2(\pi\eta) - \tau_{applied} b\eta + E_{interaction}(\eta) + E_{APB}(c,\eta) + E_{mixing}(c). \tag{8}$$

The last term in the equation corresponds to composition dependence of the heat of mixing. If the system has an ordering tendency (outside the APB) and the system has an inhomogeneous composition is actually phase-separated, then this term determines the energy penalty for such unmixing. Composition dependence of APB energy is also explicitly incorporated. Figure 2 shows the variation of E_o as a function of c, η in a model system where the high energies at of 0.5 and 1.5 correspond to the superpartial dislocations. At $\eta = 1$, the energy values correspond to the APB energy. At $\eta = 0$ the only contribution is the heat of mixing in the bulk. The system chooses the composition and slip parameter profile such that the energy is minimized with the constraint that composition be conserved.

In phase field calculations, the system is initialized according to the desired spatial distribution of c and η. The distributions of these parameters are evolved with time towards equilibrium using:

$$\frac{\partial c}{\partial t} = -M_c \nabla \cdot \left[-\nabla \left(\frac{\partial E_o}{\partial c} - 2\kappa_c \nabla^2 c \right) \right] \tag{9}$$

$$\frac{\partial \eta}{\partial t} = -M_\eta \left(\frac{\partial E_o}{\partial \eta} - 2\kappa_\eta \nabla^2 \eta \right). \tag{10}$$

κ_c is related to the penalty for having a composition gradient and this is chosen to correlate with the chemical interfacial energy, while κ_η is the penalty for having a slip parameter gradient and this is chosen to correlate with the dislocation line energy. Mobility (M) has its usual meaning in the sense that higher the mobility, the change in phase field parameter is higher for the same time-step. The mobility (M_c) in the Cahn-Hilliard equation is related to diffusivity, while mobility (M_η) in the Allen-Cahn equation is the dislocation velocity dependence on stress (reciprocal of the dislocation drag coefficient). The two evolution equations are solved simultaneously so that whatever initial state is assumed, system will tend to a final state which minimizes the overall energy. In the interest of reducing computational time, phase field evolution in this study was done in 2D, i.e., composition evolution was restricted to within the slip plane.

Since these are higher order partial differential equations in space and time, solving them analytically is difficult. Numerical techniques used in this study were the explicit Euler technique for the slip parameter evolution and semi-implicit Fourier technique [31] for the concentration evolution. The usage of Fourier method allows larger time-steps and faster so convergence to the solution is faster. Using Fourier technique requires application of periodic boundary conditions and since the slip-parameter profile across the slip plane is not periodic in our problem, we cannot directly apply Fourier technique to it. As with all numerical methods, the time step and mobility parameters were chosen such that convergence is ensured. The simulated system consisted of 50 000 pixels with the pixel width (h) being $b/4$. The values of other parameters used in this study are:

$\mu = 60\,\text{GPa}$, $\text{b} = 2.5\,\text{A}$, $\mu = 1.74$, $\text{E}_\eta|_{\max} = 6.74\,\text{Jm}^{-2}$, $\kappa_\eta = 10^{3}{*}\text{h}^2\text{J} = 3.91{*}10^{-18}\,\text{J}$, $\text{M}^*_\eta\Delta\text{t} = 10^{-4}\,\text{J}^{-1}\text{m}^2$, $\kappa_c = \text{h}^2\text{J} = 3.91{*}10^{-21}\,\text{J}$, $\text{M}^*_\text{c}\Delta\text{t} = 10^{-3}{*}\text{h}^2\text{J}^{-1}\text{m}^4 = 3.91{*}10^{-24}\text{J}^{-1}\text{m}^4$, $\tau_{\text{applied}} = 300\,\text{MPa}$.

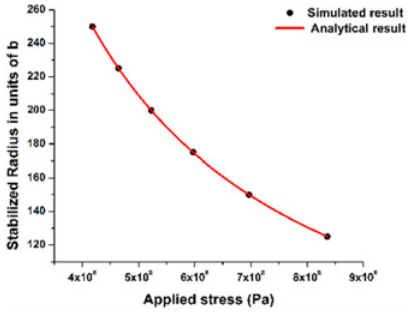

Figure 3. A comparison between simulated and analytically-solved values of radius of stable loop as a function of stress.

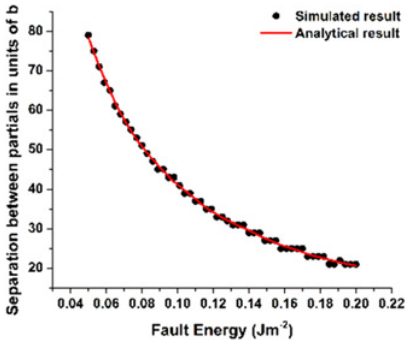

Figure 4. A comparison between simulated and analytically-solved values of separation between partial dislocations as a function of fault energy.

3. Results

3.1. Validation of model

Since this is a new phase field description of dislocations, the model was tested against classic problems in dislocations where analytical solutions are known. This is an essential exercise for validating our description of dislocation energies.

The first problem studied was the stress required to prevent the collapse of a circular dislocation loop of a perfect dislocation [16]. For this study, Eq. (4) was used in conjunction with Eq. (9). A perfect circular dislocation loop of radius, r was constructed by assigning $\eta = 0$ for the region outside the circle as this characterizes the unslipped region and $\eta = 1$ for the area inside the circle (i.e., the slipped region). When this configuration is allowed to evolve in the absence of external stress, it is seen that the dislocation loop shrinks in an attempt to minimize the line energy and eventually vanishes. However, if an external stress is applied, the loop could be stabilized at a specific final radius. The stabilized radius is plotted as a function of the applied stress in Fig. 3. Also shown is the analytical solution. It is observed that the phase field simulation is able to reproduce the analytical solution accurately suggesting that the description of line energy in the first term of Eq. (4) is accurate. The same formulation was also used to simulate Orowan looping between pinning points and these results also matched analytical solutions accurately.

The second validation test involved predicting the equilibrium separation between two superpartial dislocations for a given APB energy. In this case Eq. (5) was used along with Eq. (9). Here, $\eta = 0$ is the unslipped region, $\eta = 1$ corresponds to the APB and $\eta = 2$ corresponds to the region swept by both superpartial dislocations. Figure 4 shows the comparison between simulation results and the analytical solution. Once again, the phase field model is able to capture this phenomenon well, suggesting that the descriptions of $E_{interaction}$ and E_{APB} are good. From this we conclude that the present phase field formulation for describing phenomena involving single and pairs of dislocations is robust.

3.2. Suzuki segregation and strengthening

For studying this phenomenon a pair of superpartial dislocations separated by an APB was considered. Once again, $\eta = 0$ is the unslipped region, $\eta = 1$ corresponded to the APB and $\eta = 2$ corresponded to the region swept by both superpartial dislocations. Suzuki segregation studied in this work was on two specific pseudo-binary systems: Ni_3(Al,Ti) and Co_3(W,Al). The dependence of E_{APB} and E_{mixing} on composition (in Eq. (8)) for these systems was computed via first principles electronic structure calculations, the details of which are reported elsewhere [8], but the results are presented in Fig. 5. It is interesting to note that the two systems have different dependencies on composition and thus a difference in behavior is expected. In the following calculations a composition of 0.5 was chosen as overall the γ' composition; these are typical compositions in superalloys containing Ni_3(Al,Ti) and Co_3(W,Al) precipitates.

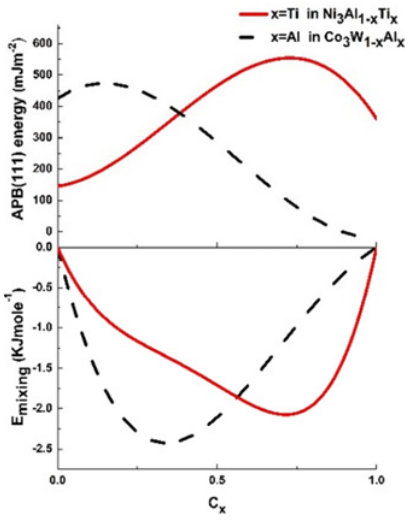

Figure 5. Composition dependence of APB energy and enthalpy of mixing in Ni_3 Al(Ta/Ti) and Co_3W(Al).

In the first set of calculations, no stress was applied. The initial composition was uniform everywhere ($c = 0.5$). A normal random noise of maximum amplitude, 0.0001 was imposed to composition distribution to mimic thermal noise. An extended superdislocation with a separation between the superpartials corresponding to the APB energy for $c = 0.5$, was introduced. With this initialization, the system was allowed to equilibrate by simultaneously solving Eqs. (9) and (10) iteratively.

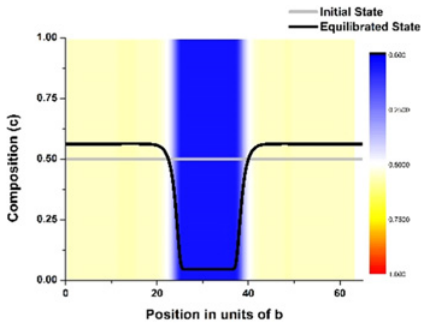

Figure 6. The initial and equilibriated concentration profiles in $Ni_3Al_{1-c}Ti_c$ alloy are superimposed on top of the composition map. The deep blue shades correspond to a low Ti concentration.

Figure 6 shows the initial and the equilibrated states in the Ni_3(Al,Ti) system. In this figure, the composition profile across the fault is superimposed on top of the composition map. The composition map is shown for the equilibrated state with the colorbar indicating the local composition. It is seen that the composition within the stacking fault is lower than outside, suggesting that Ti desegregates from the fault. This is also reflected in the concentration profile. It is also observed that the superpartial dislocations are further separated in the equilibrated condition. These effects are consistent with the predictions from Gibb's adsorption isotherm. Since APB energy is higher for higher amounts of Ti (Fig. 5), there is a desegregation of Ti from the fault. In the process of equilibrating, since the fault energy decreases, the equilibrium separation of the partials also increases.

Similar calculations were also done in the Co_3(W,Al) system. Here, it is observed that there is a segregation of Al atoms to the APB. This can once again be explained by examining the composition dependence of APB energy. Here again, as the APB is enriched in Al, its energy is lowered and the separation increases. However, our simulations also suggest that the partials continue to separate and true equilibration is never achieved. This is because, as seen in Fig. 5, APB energy is less than zero for high concentrations of Al. So, as Al enriches the fault, there is continued separation of the superpartial dislocations. Thus our simulations predict that Suzuki segregation should result in the formation of extended superdislocations. This also suggests that at high temperatures, Co_3(W,Al) precipitates may significantly weaken due to loss of order strengthening.

In the second set of simulations, an external stress was applied to a system containing a fully equilibrated fault in the case of Ni_3(Al,Ti) and for a system with uniform composition in the case of Co_3(W,Al); the latter choice was made since composition on the fault never equilibrated. The applied stress was kept constant (at 300 MPa) for all cases. A variable in this study was the non-dimensional ratio of the mobility terms $\left(\frac{1}{h^2}\frac{M_c}{M_\eta}\right)$, for the sake of convenience we refer to as 'M_r'. A low mobility ratio occurs when diffusivity is slower than the velocity of dislocations and this corresponds to low temperatures. A high mobility ratio corresponds to a condition where

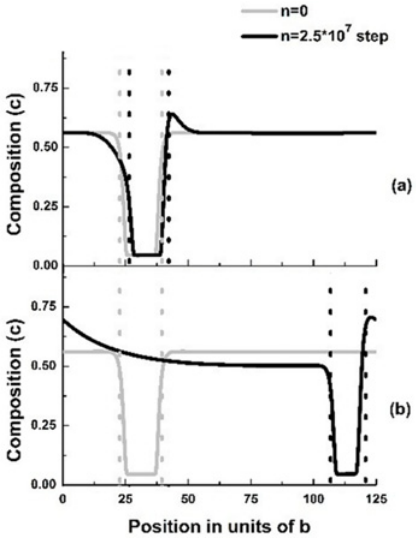

Figure 7. Concentration profile across the extended superdislocation at different times for (a) $M_r = 0.1$, (b) $M_r = 10$ for Ni_3(Al,Ti) system. Dotted vertical lines represent the position of superpartial dislocations and solid lines indicates the composition profile across the slip plane.

diffusivity rates are high compared to the dislocation velocity, a situation that can occur at high temperatures.

With this initialization, the system was again allowed to equilibrate by simultaneously solving Eqs. (9) and (10) iteratively. Figure 7 shows the composition profile and position of the superpartials at two different times and for two mobility ratios. For low M_r, the dislocation motion is significantly slower than when M_r is high. This occurs because at low M_r, when the dislocation moves in response to stress, it breaches into virgin material and a part of the stacking fault behind the leading superpartial is enriched in Ti and thus has a high APB energy. This increase in energy results in a virtual osmotic force on the leading partial that prevents it from moving forward, unless diffusion allows for the rejection of Ti back into the bulk. Such rejection of Ti is also the cause of the distortion of the concentration profile (with a pileup of Ti) ahead of the leading superpartial. Thus, in this case, the dislocation can move only as rapidly as diffusion allows it to. When M_r is high, diffusion is fast and as a result, the dislocation mobility is fast. Note that the concentration profile moves along with the pair of dislocations. Thus, in our simulations, we have been able to capture the drag phenomenon of solute (in this case, Al) atoms along with the dislocation. Simulations have also been done with applied stress as a variable (details presented elsewhere) and it is observed that at high stresses, dislocation breakaway (from solutes) phenomenon can also be captured by the model.

In the case of Co_3(W,Al), the simulation was initialized with a uniform composition everywhere. Interestingly, it is observed that for low M_r, the extended dislocation moves freely as though there was no dependence of APB energy on composition. There is no separation of the superpartial dislocations either. The composition on the fault is almost the same as the bulk composition. All these phenomena are due to lack of atomic mobility. At high

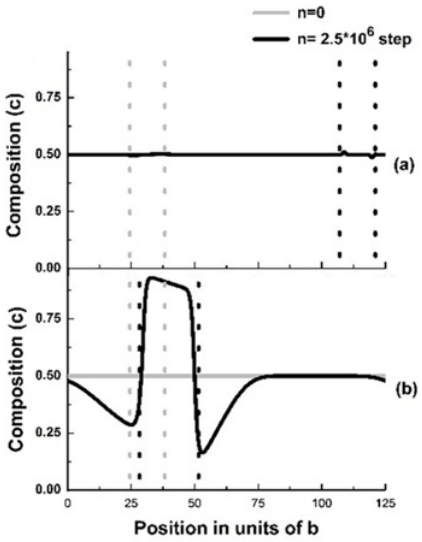

Figure 8. Concentration profile across the extended superdislocation at different times for (a) $M_r = 0.1$, (b) $M_r = 10$ for Co_3(Al,W) system. Dotted vertical lines represent the position of superpartial dislocations and solid lines indicates the composition profile across the slip plane.

M_r, the dislocation moves slower and the composition within the fault exhibits segregation. Additionally, one also observes that the separation between the superpartials increases. It is also worth mentioning that when an external stress is applied, due to competition between dislocation motion and diffusion, the APB concentration never reaches the equilibrium concentration which it would have been achieved had the dislocation been static. Due to this, the superpartial dislocations do not separate indefinitely. Instead, it is observed that the separation of the superpartials is dependent on M_r. While very high M_r, i.e., almost static dislocations, result in indefinite extension, low M_r, results in no further extension. The former case is expected at high temperatures. Thus it is likely that formation of extended superdislocations in Co_3(W,Al) will be limited to high temperatures.

4. Conclusions

A phase field model was developed to study the motion of extended dislocations in systems where planar fault energy depends on composition. The model allows for concurrent evolution of composition and dislocation position. During the motion of an extended superdislocation phenomena such as Suzuki segregation to the APB and solute drag were observed. The model also predicts that the velocity of the dislocation, under an applied stress will be sensitive to the mobility ratio, M_r.

The authors thank Prof. T. A. Abinandanan, Department of Materials Engineering, Indian Institute of Science for his valuable technical inputs and Department of Science and Technology, Government of India for their support.

References

[1] R.C. Reed, *The Superalloys* (Cambridge University Press, 2006)
[2] J. Sato, T. Omori, K. Oikawa, I. Ohnuma, R. Kainuma and K. Ishida, Science **312,** 90–91 (2006)
[3] B. Kear, H. Wilsdorf, Trans. Metall. AIME **224**, 382 (1962)
[4] T.M. Pollock and A.S. Argon, Acta Mater. **40**, 1–30 (1992)
[5] R.R. Unocic, N. Zhou, L. Kovarik, C. Shen, Y. Wang and M.J. Mills, Acta Mater. **59**, 7325–7339 (2011)
[6] B.H. Kear, J.M. Oblak and A.F. Giamel, Metall. Mater. Trans. B **1**, 2477–2486 (1970)
[7] M. Chandran and S.K. Sondhi, Modelling Simul. Mater. Sci. Eng. **19**, 025008 (2011)
[8] K.V. Vamsi and S. Karthikeyan, in Proc. Twelfth Int. Symp. Superalloys (The Minerals, Metals and Materials Society (TMS), Warrendale, PA, 2012), 521–530
[9] J. Douin, P. Veyssiere and P. Beauchamp, Philos. Mag. A. **54**, 375–393 (1986)
[10] T. Kruml, E. Conforto, B. Lo Piccolo, D. Caillard and J. L. Martin, Acta Mater. **50**, 5091–5101 (2002)
[11] H.P. Karnthaler, E.T. Muhlbacher and C. Rentenberger, Acta Mater. **44**, 547–560 (1996)
[12] D.M. Dimiduk, J. Phys. III **1**, 1025–1053 (1991)
[13] A. Korner, Philos. Mag. A. **58**, 507–522 (1988)
[14] N. Baluc, R. Schaublin, Philos. Mag. Lett. **64**, 327–334 (1991)
[15] A.P. Sutton and R.W. Balluffi, *Interfaces in Crystalline Materials* (Oxford University Press, 1995)
[16] J.P. Hirth and J. Lothe, *Theory of Dislocations*, (Wiley, 1982)
[17] H. Suzuki, Sci. Repts. Tohoku Univ. **A4**:455 (1952)
[18] Y.U. Wang, Y.M. Jin, A.M. Cuitino and A.G. Khachaturyan, Acta Mater. **49**, 1847–1857 (2001)
[19] S.Y. Hu and L.Q. Chen, Comput. Mater. Sci. **23**, 270 (2002)
[20] C. Shen and Y. Wang, Acta Mater. **52**, 683 (2004)
[21] Y. Wang and J. Li, Acta Mater. **58**, 1212–1235 (2010)
[22] S.Y. Hu, J. Choi, Y.L. Li and L.Q. Chen, J. Appl. Phys. **96**, 229–236 (2004)
[23] S.Y. Hu, Y.L. Li, Y.X. Zheng and L.Q. Chen, Int. J. Plasticity **20,** 403–425 (2004)
[24] V.A. Vorontsov, C. Shen, Y. Wang, D. Dye and C.M.F. Rae, Acta Mater. **58**, 4110–4119 (2010)
[25] Y. Koizumi, T. Nukaya, S. Suzuki, S. Kurosu, Y. Li, H. Matsumoto, K. Sato, Y. Tanaka and A. Chiba, Acta Mater. **60**, 2901–2915 (2012)
[26] P. Srimannarayana, K.V. Vamsi and S. Karthikeyan (Unpublished)
[27] L.Q. Chen, Annu. Rev. Mater. Res. **32**, 113 (2002)
[28] J.W. Cahn and J.E. Hilliard, J. Chem. Phys. **28**, 258–267 (1958)
[29] J.W. Cahn, Acta Mater. **9**, 795–801 (1961).
[30] S.M. Allen and J.W. Cahn, Acta Mater. **27**, 1085–1095 (1979)
[31] L.Q. Chen and J. Shen, Comput. Phys. Commun. **108**, 147–158 (1998)